Vertical structure of aerosol fields in the atmospheric boundary layer reconstructed from laser sensing data

Yu.S. Balin and A.D. Ershov

Institute of Atmospheric Optics,
Siberian Branch of the Russian Academy of Sciences, Tomsk

Received December 28, 1998

The behavior of vertical profiles of scattering coefficients is examined based on statistical analysis of the data obtained during whole day round lidar experiments conducted in a spring-summer period. The data were separated into subsets according to the type of air masses, season, and time of the day. The behavior of autocorrelation matrices was shown to vary with altitude whereas eigenvectors demonstrated their statistical stability. Four-layer altitude model is proposed taking into account peculiarities of behavior of the scattering coefficients' mean profiles and their statistical characteristics.

As known, vertical structure of the aerosol fields in the lower troposphere is formed under the effect of physical processes of different temporal and spatial scales, from micrometeorological to synoptic ranges of the spectrum. It causes the time duration of an experiment from diurnal to seasonal.

Investigations of the optical and microphysical properties of aerosol fields in the troposphere have been carried out during recent years principally by means of airborne instrumentation[1,2] and the ground-based laser sounding tools.[3,4] The most complete statistical data of optical observations are published in Ref. 5 where the data array is presented, which was obtained from airborne nephelometric measurements and was intended for creation of a dynamical model of the optical characteristics of atmospheric aerosol. Such a model is based on the peculiarities of diurnal, seasonal, and annual behavior of the scattering coefficient at different altitudes, including the dependence on the type of air mass.

Though having the undoubted scientific significance of such investigations, especially for large spatial scales, one should note their principal disadvantage related to organization of airborne observations. First of all, this means great time discreteness of measurements along the vertical direction in different time of day, especially at small altitudes in the nighttime.

In this paper, which is based on the conception proposed in Ref. 5, we consider the behavior of the vertical profile of the scattering coefficients in different time of day and under different synoptic conditions with more fine spatial and temporal resolution.

We use the data of sounding at the wavelength 0.53 μm obtained in spring and summer (April–June) 1993 by means of a LOZA–3 lidar in the city of Tomsk. Measurements were performed round-the-clock every two hours. The lidar sounded the atmosphere both in horizontal and vertical directions up to 2 km with the spatial resolution of 15 m. Thus, 12 vertical profiles of aerosol scattering coefficients were obtained every day.

Let us briefly consider the peculiarities of synoptic and meteorological conditions of the atmosphere during the period of this experiment. The temporal diagram of the change of air mass is shown in Fig. 1, and the occurrence (%) of the principal synoptic objects during the period under study is given in Table 1.[6]

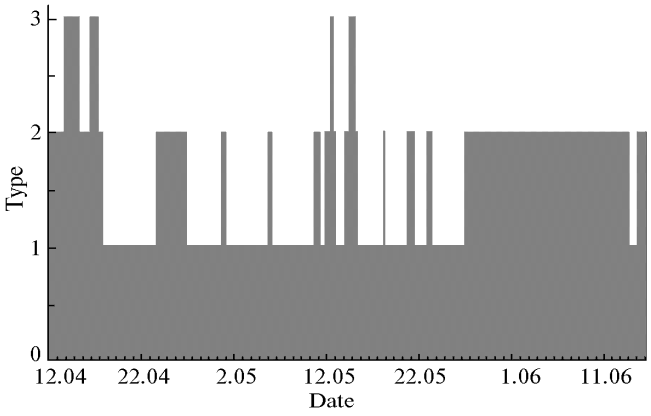

Fig. 1. Temporal diagram of the change of air mass during the experiment.

According to data of many-year observations in West Siberia, the main contribution (60%) to the formation of synoptic situations comes from midlatitude continental air mass.[7] It is approximately the same statistics (52%) that was observed in the experimental study considered. It is important that in the first half of the period of observations the main contribution came from the Arctic air mass, while in the second half the continental polar air mass dominated.

As for the statistics of the occurrence of principal synoptic situations presented in Table 1, it differs, for May, from many-year one in which an insignificant peak of cyclonic activity is normally observed.[7]

0235-6880/99/07 592-08 $02.00

Table 1. Frequency of occurrence (%) of the principal synoptic objects

Month	Cyclone	Anticyclone	Front	Contrast zone	Small-rate field	Fronts + Cyclones
IV	18	38	22	6	24	31
V	27	35	20	14	5	47
VI	33	16	8	3	40	41

The variety of synoptic conditions allows us to examine the possibility of describing the general form of the vertical distribution of the scattering coefficient, because the statistical lidar data on the behavior of the aerosol scattering coefficient are very limited and mostly are only illustrative.[3] In particular, the three-layer altitude model has been proposed in Ref. 4, but these data were obtained only in anticyclones in nighttime, and so they do not reflect the whole pattern.

Figure 2 shows the monthly mean diurnal behavior of the vertical distribution of the aerosol scattering coefficient. In general, the behavior of the profiles in the aforementioned months is similar. As one should expect, the greatest altitude gradient is observed in the near-ground layer of the atmosphere, where the effect of diurnal behavior is also well pronounced. The diurnal variability in spring (April and May) is characterized by sharp maxima in the lower layers. As follows from the synoptic situation (see Table 1 and Fig. 1), it is possibly caused by a frequent change of air mass and insufficient heating of the boundary layer. One should note that the maximum of aerosol scattering coefficient in April is observed at 1 p.m., while in May the first maximum is at 9 a.m. and the second one at 7 p.m. The mean diurnal behavior of the aerosol number density obtained in the ground layer near Novosibirsk in summer is quite similar.[8] The evening maximum in 1991 has a lower amplitude, but in the data of 1993 it forms the main peak. Since the increase of aerosol number density correlates with the solar radiation, the authors of Ref. 8 have drawn the conclusion that the fine particles generated in photochemical transformations make up the principal aerosol fraction that leads to the first maximum.

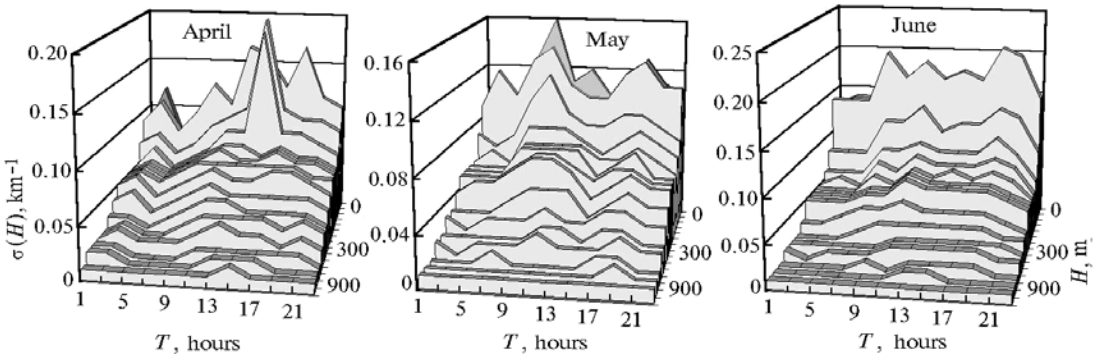

Fig. 2. Mean diurnal behavior of the vertical distribution of the scattering coefficient in different months.

Summer period represented by measurements in June is the most characteristic of the whole measurement cycle. In order to consider the dynamics of diurnal behavior of the vertical profile of aerosol scattering coefficient in a more detail, let us select the data array with the minimum observed values of the aerosol scattering coefficient $\sigma(H)$. As follows from Fig. 2, these are the values obtained at 1 a.m.

Figure 3 shows the temporal dependences $\Delta\sigma(H, t) = \sigma(H, t) - \sigma(H, 01)$, which characterize the mechanism of transformation of the profiles during a day. In summer, in the evening and nighttime, the near-ground temperature inversion is usually formed.[9] Its altitude reaches 400–500 m in the morning.

According to the formed dependence, the function $\Delta\sigma(H, 01)$ takes zero value within the whole altitude range. As follows from two next measurements, the altitude of 400–500 m is the boundary, above which the value $\sigma(H)$ is less than $\sigma(H, 01)$, and below it σ is greater than $\sigma(H, 01)$. Sunrise is the trigger for the processes of turbulent exchange, generation of "new" aerosol, and aerosol emission from the underlying surface to the above layers. The first stage of this process is represented by measurements at 7 a.m. One can see a significant increase in the scattering coefficient in the near-ground layer and formation of a peculiar section boundary at the altitude of 600 m, where $\sigma(H)$ already exceeds its nighttime values (compare with the data on $\Delta\sigma(H, 03)$ and $\Delta\sigma(H, 05)$). Probably, the increase of $\sigma(H)$ at these altitudes at this time of day is caused by dominating processes of photochemical and chemical gas–to–particle transformations. The aerosol emission processes dominate in the lower part of the atmosphere. The next measurement performed in 2 hours confirms this hypothesis. It is characteristic that the section

boundary (~ 600 m) exists as before, indicating the presence of temperature inversion or the layer with a stable stratification.

On the whole, the spatiotemporal dynamics of vertical distribution of the aerosol scattering coefficient coincides with the diurnal behavior of the thermal regime of the atmospheric boundary layer in the midlatitudes in summer.[9] Air temperature quickly increases in the morning and reaches its maximum values at 1–2 p.m. Then it slowly decreases with the increase in the gradient since 5 p.m. until sunset. It is observed in the altitude behavior of $\sigma(H)$ so that the maximum values of the scattering coefficient in the near-ground layer, intensive filling of the lower under-inversion layer, and its penetration into the above layers are observed at 11 a.m. Then this process continues until 1 p.m. The evidence of this fact is the decrease in the scattering coefficient up to 600 m and its increase in the layer up to 1200 m.

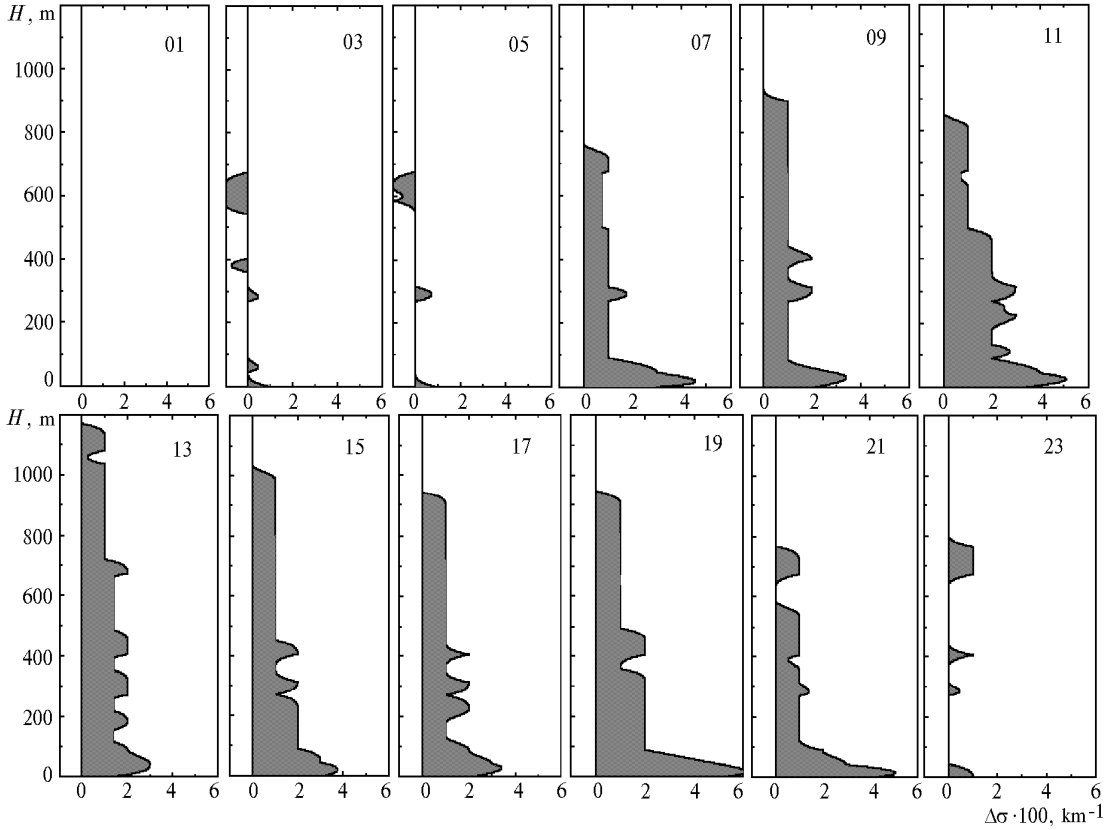

Fig. 3. Mean diurnal behavior of the vertical distribution of the relative values of the aerosol scattering coefficient $\Delta\sigma(H, t)$ in June. The basis profile is that obtained at 1 a.m.

As is seen in Fig. 2, the diurnal behavior practically does not affect the scattering coefficient at these altitudes. This dependence correlates with the diurnal behavior of temperature. The amplitude of temperature oscillations at these altitudes decreases by more than 5 times relative that in the near-ground layer,[9] that, by the way, defines the term "boundary layer."

The described mechanism of transformation of the vertical profile of the aerosol scattering coefficient lies in the frameworks of the concept on the presence of the principal (PML) and internal (IML) mixing layers in the atmosphere. As follows from this concept examined on the basis of data on the aerosol number density, the aerosol generated in the near-ground layer is firstly accumulated inside the IML and then it penetrates to the principal mixing layer.[10]

Since 3 p.m. the intensity of turbulent exchange decreases, and the section boundary appears at the altitude of 600 m. The upper layers are destroyed, and the accumulation of aerosol is observed in the lower layers. It reaches the maximum value at 7 p.m. Thus, two maxima are observed in the diurnal behavior, at 11 a.m. and 7 p.m. In the evening generation of new particles, due to photochemical reactions and aerosol emission from the near-ground layer stop. Simultaneously their sedimentation to the ground surface occurs, and, hence, the atmosphere is cleaned.

Considering the presented vertical distributions of the aerosol scattering coefficient together with the vertical behavior of the variance, one can reveal the characteristic altitude ranges, where the transformation of the diurnal behavior is observed. Figure 4 shows the vertical profile of the variation coefficients of $\sigma(H)$ for two opposite moments of a June day: daytime (1 p.m.) and night (1 a.m.). As is seen from Figs. 3 and 4, there are some nodes which divide the altitude ranges in the atmosphere by the dynamics of their optical properties. In this case, the characteristic nodes are at the following

altitudes: near-ground layer of the atmosphere (~ 200 m), internal mixing layer (~ 600 m), and the principal mixing layer (~ 1200–1400 m).

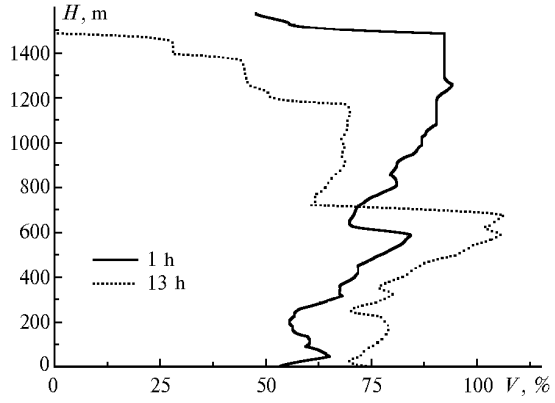

Fig. 4. Vertical profile of $\sigma(H)$ variations.

For quantitative estimation of the relationships between the optical parameters of the atmosphere at different altitudes, let us consider statistical characteristics of the profiles $\sigma(H)$. Let us carry out the statistical analysis on the basis of autocorrelation matrices and systems of their eigenvectors, that makes it possible to use the method of optimal extrapolation of the altitude behavior of $\sigma(H)$ in the following form[11]:

$$\sigma(H) = \bar{\sigma}\ (H) + \sum_{k=1}^{m} C_k(\sigma)\ F_k(H)\ ,$$

where $C_k(\sigma)$ are the coefficients of expansion over the eigenvectors, m is the number of eigenvectors used in reconstruction of the profiles. If only the first eigenvector has been used, we have a single-parameter model, and the problem is in finding the relations between $C_1(\sigma)$ and easy measurable parameters of the medium, which are the input parameters to the model.

It is proposed in Ref. 12, to use the scattering coefficient in the near-ground layer of the atmosphere and/or the optical thickness as input parameters for realizing the procedure of reconstruction. It is the way used in one of the first Elterman's models.[13] For refining the model one can use subsequent expansions. The authors of Ref. 12 relate the variations of $\sigma(H)$ to the integral characteristics of air temperature in the near-ground layer of the troposphere as a whole, and demonstrate the efficiency of such an approach by histograms of distribution of the relative errors in reconstructed vertical profile of the aerosol scattering coefficient in different seasons.

When analyzing the properties of optimal representations of the vertical profile of the aerosol scattering coefficient, one should pay attention to the character of their statistical stability, i.e., to the types of distributions in different meteorological situations. So, analysis of the statistical characteristics was carried out both for the data array as a whole and with dividing according to the features taking into account the greatest variations of $\sigma(H)$. First of all, it is the seasonal variability considered according to the calendar principle, variability inside a season, i.e., analysis of the types of air mass, diurnal dependence, i.e., the daytime and nighttime periods. The quantitative parameters of the data arrays formed in that way are presented in Table 2.

Table 2

Data Array	Number of measurements	Ratio to the total number, %
Daytime (7.00–19.00)	363	56
Nighttime (21.00–5.00)	280	44
April	188	29
May	301	47
June	154	24
Arctic type of air mass	331	51
Midlatitude type of air mass	287	45
Whole array	643	100

Correlation matrices and the system of eigenvectors were calculated up to 1500 m with the spatial resolution of 30 m. Let us first consider the behavior of autocorrelation matrices depending on the season (Fig. 5). It is seen that the altitude dependences change at the transition from spring measurements to the summer ones. The uniform change of the correlation coefficient with altitude is characteristic of April, while in May the altitude of 600 m can be noted, where all curves are concentrated. Thus, the area below this boundary, where the values of the aerosol scattering coefficient at all altitudes are well correlate with each other ($R \geq 0.5$).

An approach was proposed in Refs. 1 and 5 for the objective estimation of the mixing layer height. The approach is based on the data of airborne measurements of optical and microphysical characteristics of aerosol and lies in finding the altitude of the correlation destruction. As authors of Ref. 5 note, it is more correct to call this altitude "the height of correlation layer." They propose to take the altitude where the correlation coefficient $R(\sigma_0, \sigma_H)$ decreases down to 0.5 as the estimate of this height.

In our case (spring months), the first boundary value corresponds to the height of 600 m, i.e., the height of the internal mixing layer. Above this boundary, the variations of the correlation coefficient behavior are observed as characteristic concentration of lines near 1500 m in April and 1300 m in May. In June the correlation coefficients have large values in all the altitude range considered because of good turbulent exchange between the layers. The boundary value is 1300 m. In Ref. 15 we have presented the correlation matrices obtained based on measurements of June 1995, which are similar to the described one. This is an evidence of some statistical stability of the correlation matrices for summer.

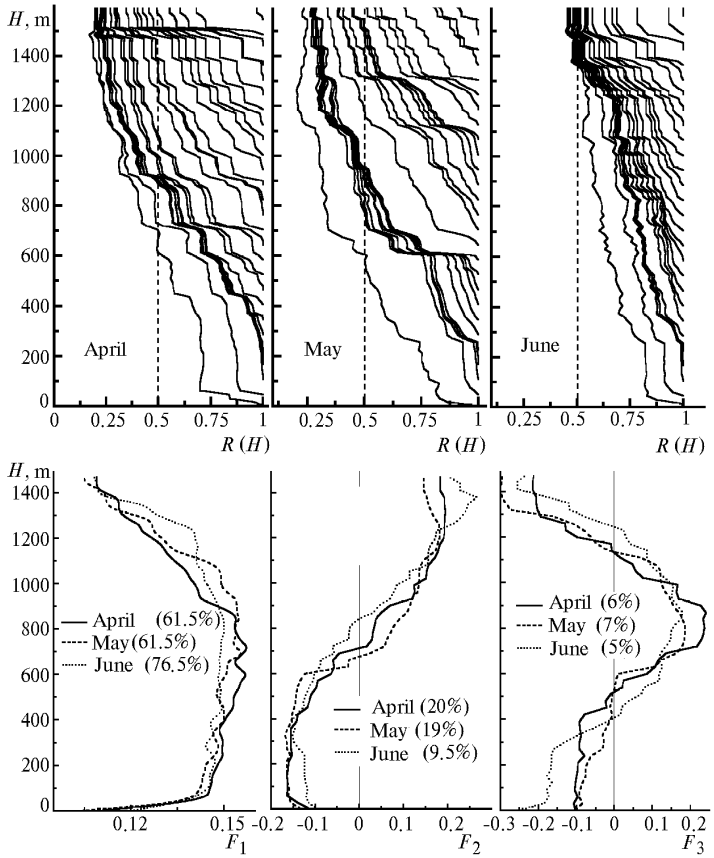

Fig. 5. Autocorrelation matrices (upper part) and the systems of their eigenvectors F_k (lower part) for different months of observations.

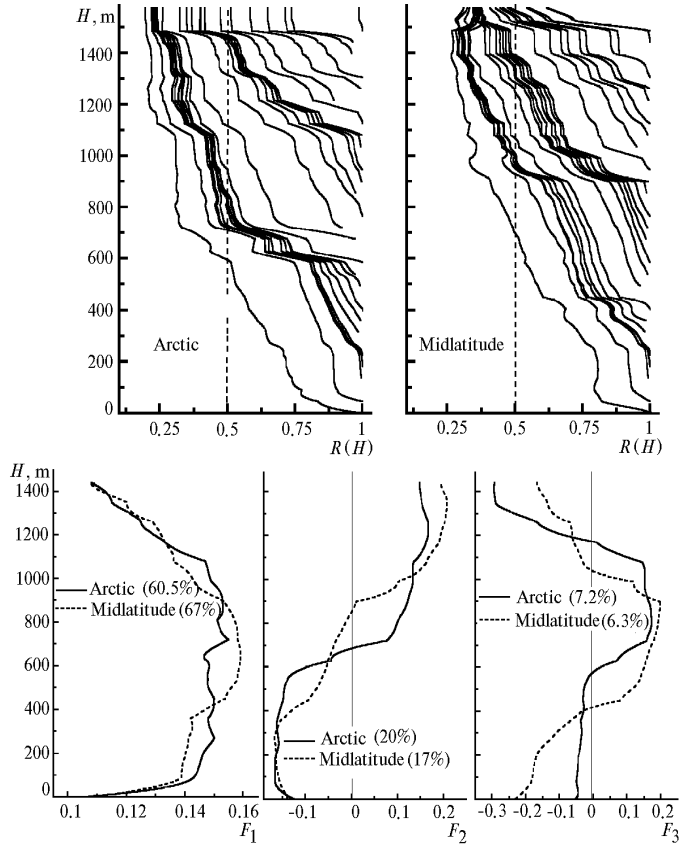

Fig. 6. The same as in Fig. 5 depending on the type of air mass.

Then the realizations were selected from the data array, which correspond to the Arctic and continental polar type of air mass. As is seen from Fig. 6, in general the behavior of correlation coefficients is analogous to that considered above. It is well seen from comparison of the matrices of May cycle and Arctic type of air mass. One can easy explain this fact, because the weather in this period was determined just by this type (see Fig. 1) of air mass.

If we consider the entire set of measurements shown in Fig. 7, one can see a more or less uniform altitude distribution of the correlation curves with the characteristic features peculiar to May cycle of measurements. Most likely, as it follows from Table 2, this is explained by a larger bulk of data compiled during this period compared to other months. The data for daytime (7 a.m. till 7 p.m.) and nighttime (9 p.m. until 5 a.m.) conditions are also shown in this figure. The variations of matrices are significantly different. In the daytime, the first altitude where $R(\sigma_0, \sigma_H) = 0.5$ is 400 m, and the concentration of lines, which determine the height of the internal mixing layer, is observed at 600 m. A 100 to 150-m-thick layer is observed at higher altitudes, where the correlation coefficient is practically constant.

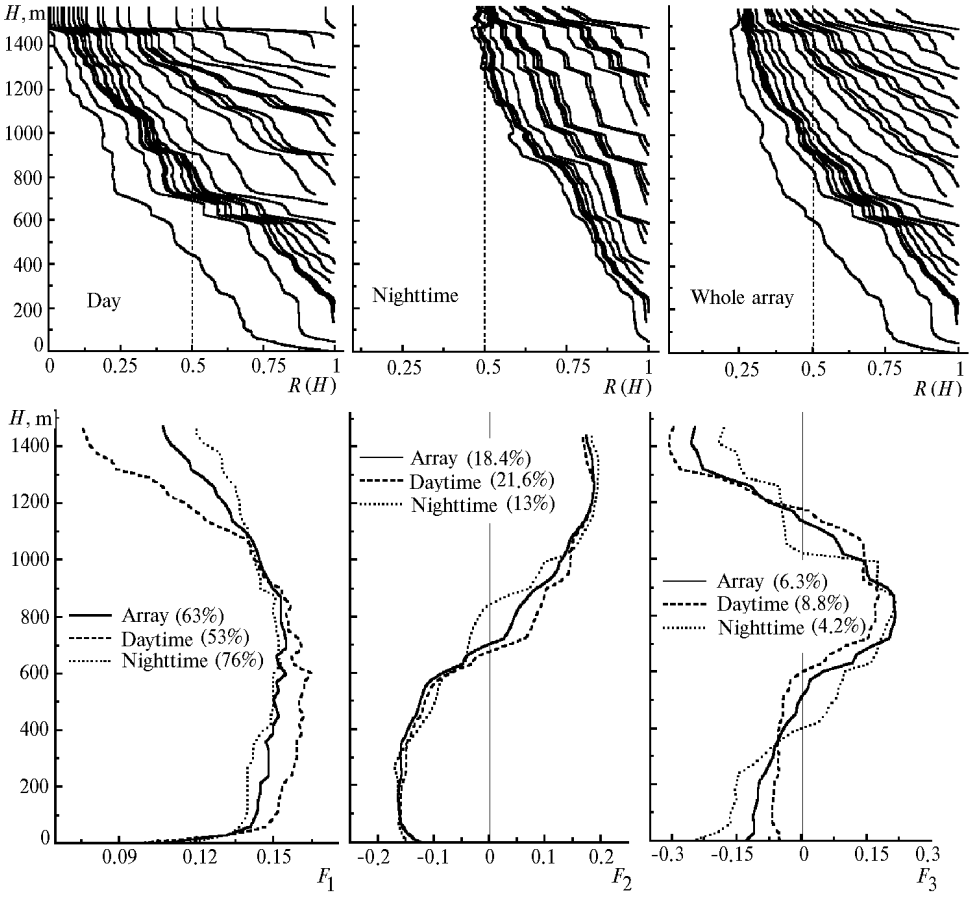

Fig. 7. The same as in Fig. 5 for daytime and nighttime conditions. The right-hand part of the figure shows the generalized data of the entire array of measurement data.

The subsequent altitude range 800–1200 m, at the upper boundary of which $R(\sigma_{0.8}, \sigma_{1.2}) = 0.5$, is characterized by good correlation of $\sigma(H)$. The adherent layer of 200 to 300 m thickness is observed above this boundary, where the correlation coefficient weakly changes with the altitude increase.

No peculiarities are observed in the nighttime conditions. Good correlation occurs at all altitudes. The first altitude where the dependences cross the level $R(\sigma_0, \sigma_H) = 0.5$ is ~ 1200 m.

On the whole, as is seen from Fig. 7, the behavior of the generalized correlation matrix is primarily determined by the character of the dependences characteristic of daytime.

Let us consider now the peculiarities in the parameters of expansion of the vertical profiles $\sigma(H)$ represented in the form of three first eigenvectors in the lower panels of Figs. 5 to 7. The fact that these vectors are obtained in different seasons, synoptic and meteorological situations, allows us to assess their statistical stability. First of all, the similarity of the first eigenvectors F_1 and two next ones is an evidence of this fact. The quantitative estimates of the accumulated variance of the vector in percent of the

matrix spur are shown in all figures next to the data array name (month, day, mass), for convenience.

As all vectors have similar character, let us analyze the parameters of the series expansion of the generalized correlation matrix (see Fig. 7).

The relative value of the accumulated variance for three vectors reaches 88% for all situations that took place during the experiments, that is an evidence of good convergence of the expansion of random profiles $\sigma(H)$ over natural orthogonal functions. The same applies to the daytime observations, while at nighttime the total variance of the expansion already reaches 93%.

As is seen from Fig. 7, the profiles of the fundamental harmonic weakly change as the altitude increases above the near-ground layer up to the mixing layer height. Let us note that the first eigenvectors F_1 describe the most characteristic variations of the aerosol scattering coefficient from the mean profile, following the altitude behavior of the corresponding rms errors. In principle, it allows one to apply the method of optimal parameterization to our problems. The main variations of the vector F_1 components are observed in the near-ground layer and at the upper boundary of the mixing layer.

The next eigenvectors take into account more fine structure of the variations of $\sigma(H)$ and also are characterized by significant stability, only weakly changing under different conditions of the experiment.

The main peculiarity of the second eigenvector is the presence of two diffuse maxima of its components of the opposite signs, in the near-ground layer and at the level of 1200 m, and a single transition through zero at a height near 600 m.

The third eigenvector is characterized by two transitions across zero line, the upper of which is at the boundary of the principal mixing layer, and by a single extremum at the boundary of the internal mixing layer. The interesting peculiarity is observed here: the extreme value of F_3 corresponds to the transition of F_2 through zero. The same peculiarity is observed in the behavior of the vectors of the correlation matrix of humidity,[16] that is one evidence more of the close relation of the aerosol scattering coefficient with the humidity field.

It follows from analysis of all data shown in Figs. 5 to 7 that the smallest variance value for F_1, equal to 53%, occurs at sounding during daytime. Obviously, in this case one can not restrict oneself to a single-parameter model, and it is needed to attract the harmonics of higher orders and to find the correlation between the expansion coefficients and optical and microphysical parameters of the atmosphere, for example, as it is proposed in Ref. 14.

It is worth noting here that the obtained eigenvectors F_k for the aerosol scattering coefficient are in a qualitative agreement with that for the profiles of lidar ratio[17] and the backscattering coefficient[18] in the lower troposphere.

Thus, considering all the material as a whole, one can propose a scheme of a four-layer vertical distribution of the vertical profile of the aerosol scattering coefficient in the lower troposphere. It is shown in Fig. 8 and includes the node heights, on which the three-layer model of $\sigma(H)$ is based,[4,12,19] while adding the height H_{IML} – the internal mixing layer boundary.

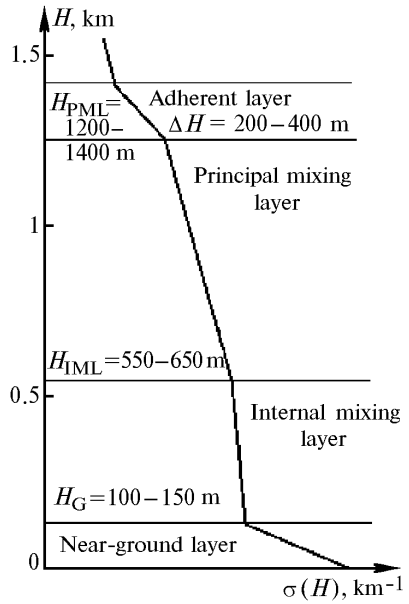

Fig. 8. Schematic representation of the vertical profile of the aerosol scattering coefficient.

The node heights H_G, H_{IML}, and H_{PML} were determined based on variations of both mean profiles $\sigma(H)$ and their statistical characteristics. There are many papers devoted to the aerosol behavior in the selected height regions (see, for example, the references in this paper). Nevertheless, when considering the proposed scheme, we would like to mention one moment related to the definition of the mixing layer. There is a special paper[10] in the literature devoted to this question, where the review is presented of some available approaches to determining H_{PML}, which show the ambiguity of this term. The authors of Ref. 10 suggest, on the basis of airborne measurements of the aerosol number density, to determine H_{PML} by the break of correlation. At the same time, as was correctly noted in Ref. 14, the aerosol processes are inertial and the height H_{PML} calculated from the aerosol data differ from that determined by the turbulent exchange intensity.

Moreover, assuming a correct statement of the problem, one should take into account the peculiarity of aerosol measurements and the processes aerosol may take part in. The authors of Ref. 5 obtained the estimate $H_{PML} \sim 3$ km from analysis of the scattering

coefficients of dry aerosol matter. The principal reason of the difference from our data is in taking into account the effect of relative humidity. If to reduce the profiles of the dry matter to the real value of humidity, as was done in Ref. 5, the rate of decrease of the correlation coefficient is significantly greater. This leads to a decrease in the determined H_{PML}. The instrumental realization of the experiment plays an important role either, because the lidar and the nephelometer[5] have different sensitivity to variations in concentration and the size spectrum of aerosol particles.

Finally, each of atmospheric parameters has its own "height of correlation," although the processes of formation of its vertical structure have common nature.

Acknowledgments

In conclusion, the authors would like to thank the staff of the Laboratory of Optical Sounding of Aerosol of the Institute of Atmospheric Optics, who provided a valuable help in carrying out round-the-clock lidar observations.

The work was supported in part by the Russian Foundation for "asic Researches (grants No. 98–05–031777 and 98–05–64263).

References

1. Yu.D. Kopytin, ed., *Spatial-Temporal Variability of the Characteristics of Atmospheric Aerosol* (Nauka, Novosibirsk, 1989), 152 pp.
2. V.E. Zuev, B.D. Belan, D.M. Kabanov, et al., Atmos. Oceanic Opt. **5**, No. 10, 658–663 (1992).
3. Y. Sasano, J. Meteorol. Soc. Japan **63**, No. 3, 419–435 (1985).
4. Yu.P. Dyabin, M.V. Tantashev, S.O. Mirumyants and V.D. Marusyak, Izv. Akad. Nauk SSSR, Fiz. Atmos. Okeana **13**, No. 11, 1205–1211 (1977).
5. M.V. Panchenko and S.A. Terpugova., Atmos. Oceanic Opt. **7**, No. 8, 552–557 (1994).
6. V.G. Arshinova, B.D. Belan, and T.M. Rasskazchikova, Atmos. Oceanic Opt. **8**, No. 5, 380–385 (1995).
7. Ts.A. Shver, ed., *Climate of Tomsk* (Gidrometeoizdat, Leningrad, 1982), 176 pp.
8. P.K. Kutsenogii, Atmos. Oceanic Opt. **7**, No. 8, 563–565 (1994).
9. L.T. Matveev, *Course of General Meteorology. Atmospheric Physics* (Gidrometeoizdat, Leningrad, 1984), 751 pp.
10. B.D. Belan, Atmos. Oceanic Opt. **7**, No. 8, 558–562 (1994).
11. A.M. Obukhov, Izv. Akad. Nauk SSSR, Ser. Geofiz. **1**, No. 3, 432–439 (1960).
12. M.V. Panchenko and S.A. Terpugova., Atmos. Oceanic Opt. **9**, No. 12, 989–996 (1996).
13. L. Elterman, Report AFCRL-70-0200 Bedford Mass (1970), 68 pp.
14. M.V. Panchenko, S.A. Terpugova, and V.V. Pol'kin, Atmos. Oceanic Opt. **11**, No. 6, 532–539 (1998).
15. Yu.S. Balin and A.D. Ershov, Atmos. Oceanic Opt. **9**, No. 7, 603–611 (1996).
16. V.E. Zuev and V.S. Komarov, *Statistical Models of Temperature and Gas Components of the Atmosphere* (Gidrometeoizdat, Leningrad, 1986), 264 pp.
17. Yu.S. Balin and I.V. Samokhvalov, Izv. Akad. Nauk SSSR, Fiz. Atmos. Okeana **19**, No. 9, 937–943 (1983).
18. G.I. Gorchakov, O.K. Kostko and G.A. Krikunov, Izv. Akad. Nauk SSSR, Fiz. Atmos. Okeana **17**, No. 10, 1048–1055 (1981).
19. K.Ya. Kondrat'yev, ed., *Aerosol and Climate* (Gidrometeoizdat, Leningrad, 1991), 542 pp.